ANNALI DI GEOFISICA, VOL. 44, N. 1, February 2001

Strain pattern of the Southern Tyrrhenian slab from moment tensors of deep earthquakes: implications on the down-dip velocity

Giulio Selvaggi
Istituto Nazionale di Geofisica e Vulcanologia, Roma, Italy

Abstract
Seismic strain is analysed along the slab face of the Southern Tyrrhenian subduction zone using focal mechanisms of deep earthquakes which occurred in the period 1960-1998. Results show that the slab is mostly affected by down-dip shortening which strongly increases below 250 km depth. Extensional strain is mainly confined to the direction perpendicular to the slab face. The dominance of down-dip shortening and the minor along strike inplane extension implies thickening of the slab below 250 km depth. Assuming constant seismic efficiency along the slab, this strain pattern also implies a decrease of the down-dip velocity below 250 km depth. We also locate lower magnitude intermediate-depth and deep earthquakes using arrival times since 1985 available from the Italian seismic national network. These data show that the slab reaches the deeper part of the upper mantle, as suggested by the occurrence of a few ≈ 600 km depth earthquakes, and that a large portion of the Tyrrhenian slab, between 100 and 250 km depth beneath the offshore of the Calabrian arc, is aseismic. Only a short part of the Tyrrhenian slab is seismically continuous from the top to the bottom. The lack of seismicity may indicate either that aseismic subduction is occurring or that the slab is detached from its upper part. Although the data are still inconclusive, they suggest that an aseismic subduction is the most appropriate interpretation, considering recent tomographic images of the slab and the results of this study, which agree well with the presence of a neutral down-dip stress zone, as also observed worldwide in deep slabs.

Key words *Southern Tyrrhenian – seismic strain rate tensor – down-dip velocity – aseismic subduction*

1. Introduction

The Western Mediterranean is a broad back arc basin resulting from the fast south-eastward retreat of the subduction front that, extending from the Alps to the Betic arc, started migrating about 25 million years ago (Doglioni *et al.*, 1997). The subduction came to an end in the North Africa margin, that is currently undergoing compression due to continental collision, while the Apennines are characterised by a complex pattern of subduction where both detached slabs or subduction of continental crust has been proposed (Amato *et al.*, 1993; Spakman *et al.*, 1993; Lucente *et al.*, 1999). The Southern Tyrrhenian subduction zone, the seismically deepest of the whole Alpine-Himalayan belt, is probably the only region where the subduction of old oceanic crust (Ionian lithosphere) has still maintained the same characteristics since the early beginning of the process. Thus, this region

Mailing address: Dr. Giulio Selvaggi, Istituto Nazionale di Geofisica e Vulcanologia, Via di Vigna Murata 605, 00143 Roma, Italy; e-mail: selvaggi@ingv.it

is the obvious candidate to infer insights on the kinematics that have driven the opening of the Western Mediterranean and could provide important constraints on the dynamic of the ongoing process. Aim of this paper is to derive and discuss the strain pattern of the subducting Ionian lithosphere deduced from fault plane solutions of the intermediate and deep earthquakes which have occurred in the past 40 years. In fact, the deformation accommodated by earthquakes is the only direct information on the kinematics of the subducted slab, although its interpretation is far from being simple (Vassiliou and Hager, 1988; Holt, 1995; Nothard *et al.*, 1996). The motivation of this analysis derives from the consideration that the mode of deformation of the Tyrrhenian slab can provide independent constraints on the characteristics retrieved by tomographic images, particularly as concerns the slab thickening observed between 300 and 400 km depth (Cimini, 1999; Lucente *et al.*, 1999), and the mechanical situation of the subducting Ionian lithosphere. Furthermore, the joint interpretation of tomography and strain pattern will constrain the stress field or force system responsible for the ongoing processes.

2. Method

Seismic moment tensor of earthquakes smeared out within a lithospheric volume provides information on the average strain rate in the volume and in the period of time under study (Kostrov, 1974; McKenzie and Jackson, 1983; Jackson and McKenzie, 1988). The strain rate tensor is the symmetric part of the velocity gradient tensor, that completely describes the kinematics in the same domain (Fung, 1965; Haines, 1982; England and Houseman, 1986; Jackson and McKenzie, 1988; Holt, 1995). It follows that the thickening, shortening and extension rates of an actively deforming region can be obtained from the diagonal elements of the strain rate tensor. On the assumption that the off-diagonal components of the velocity gradient tensor can be neglected, diagonal strain rate components can supply information on the velocity field along principal directions. In this case, in a reference system where the x axis is aligned with the down-dip direction of a subducted slab, the shortening (or extension) rate is completely determined from the $\dot{\varepsilon}_{xx}$ component of the strain rate tensor and, when averaged on the total length of the slab, it provides a description of the seismic part of the down-dip velocity gradient.

This paper first discusses update locations of the intermediate and deep seismicity of Italy recorded by the Centralised Italian National Network (RSNC) to derive the main geometric features of the subducting slab. The second part calculates the state of strain deduced from available fault plane solutions of the larger earthquakes and, finally, discusses the implications of the strain pattern in terms of down-dip velocity, following the approach outlined above.

3. Intermediate and deep seismicity of the Italian peninsula

Deep and/or intermediate depth earthquakes occur only in two well distinct regions of the Italian peninsula, namely the Northern Apenninic arc (Selvaggi and Amato, 1992) and the Southern Tyrrhenian Sea (Selvaggi and Chiarabba, 1995, and references therein). Although the Northern Apennines are outside the scope of the present study, it is worth recalling the main features delineated but the intermediate seismicity because of the larger data set available today (from 1985 to 1999) and the occurrence of the largest event ever recorded in this region (March 26, 1998), and, more important, to verify the lack of intermediate depth seismicity in the Central and Southern Apennines, that is one of the major problems in inferring the continuity of the subduction process throughout Italy. The subcrustal earthquakes of the Northern Apennines are located mainly beneath the chain, north of latitude 43°, following the highest elevations, while some of them are located beneath the external foothills. They are confined down to $\approx$ 90 km depth and are not clustered in any particular depth interval but are continuously distributed at all depths. The distribution of the intermediate-depth events (sections A, B, C of fig. 1) shows that they deepen from the Adriatic Sea towards the Tyrrhenian delineating a $\approx$ 45°,

≈ 50 km wide, dipping slab. This subcrustal seismicity has been interpreted as further evidence of the subduction of the Adriatic lithosphere beneath the Apennines (Selvaggi and Amato, 1992). The width of the seismic zone enhances part or all the thickness of the Adriatic lithosphere. No further indications are derived from the few fault plane solutions available but only a generic similar compressive mechanism, involving down-dip tension. The largest fault plane solution of fig. 1 is the M_w 5.4 event which occurred on 26th March 1998. The continuity of the subduction process through the Central and Southern Apennines to the well established Southern Tyrrhenian subduction zone is still an open question because of the lack of any evidence of intermediate and deep seismicity and of clear velocity anomalies in these two regions. The latter observation, although in favour of a discontinuity of the process along the Apennines (the slab window in Amato *et al.*, 1993), does not exclude that continental aseismic subduction may occur. In this case, the signature of the slab could be weak on tomographic images.

Much more studied is the distribution of deep earthquakes in the Southern Tyrrhenian zone. The seismicity data set analysed in this paper covers 15 years of instrumental earthquakes recorded by the Centralised Italian National Network.

Locations have been obtained using a 1D velocity model (IASP91) and the location program Hypoinverse (Klein, 1989). Out of about 800 intermediate-depth and deep earthquakes located, almost 300 events can be considered well located, taking into account azimuthal gap, number of recording stations and formal errors.

Some new and original features are found, out of the previous findings reported in the recent papers published in the past (see Selvaggi and Chiarabba, 1995, and references therein for a review). In the along-strike section D of fig. 1 the deep seismicity is continuous only in a limited sector (100 km wide) of the slab while a large fraction of it, between 100 and 250 km depth, appears to be aseismic. This feature has not been observed before and will be discussed later.

Earthquakes shallower than 100 km depth are located mainly beneath the Ionian side and the Calabrian arc delineating the almost subhorizontal Ionian lithosphere. The distribution of the deeper seismicity (below 100 km) shows an abrupt change in the dipping Ionian lithosphere to an angle of about 70° or more, offshore the Calabrian arc at about 100 km depth (section E in fig. 1). The seismogenic thickness of the Ionian lithosphere, as can be seen from fig. 1E, is roughly 50 km, thus comparable with the thickness of the seismic part of the Adriatic lithosphere beneath the Northern Apennines. The occurrence of deeper earthquakes in the Tyrrhenian subduction zone has been only partly described in the past. In the updated data set analysed in this paper a few earthquakes as deep as 500-600 km have been located. These very deep earthquakes have been recorded by more than 60 stations of the Italian network and result well located (few kilometers of errors in horizontal and vertical coordinates and small azimuthal gap) with respect to the adopted velocity model. The possible influence on the location of these earthquakes of lateral heterogeneity, persistently observed in all the tomographic images, can be treated using a 3D ray-tracer and will be part of a future analysis, although in the paper of Selvaggi and Chiarabba (1995), the differences between 1D and 3D locations were limited to at least few tens of kilometers, thus negligible at the scale of our observation.

4. State of strain of the Southern Tyrrhenian subduction zone

The data set contains 57 reliable fault plane solutions of earthquakes with body wave magnitude ranging from 4.0 to 6.2 which occurred in the past 40 years. The m_b = 7.1, 1938 earthquake, whose focal mechanism has been re-evaluated by Anderson and Jackson (1987), has been included. Fault plane solutions of the largest earthquakes are available from the extensive bibliography (Gasparini *et al.*, 1982; Iannaccone *et al.*, 1985; Anderson and Jackson, 1987; Giardini and Velonà, 1990; Frepoli *et al.*, 1996, CMT solutions, and this study). The fault plane solutions extracted from existing literature have

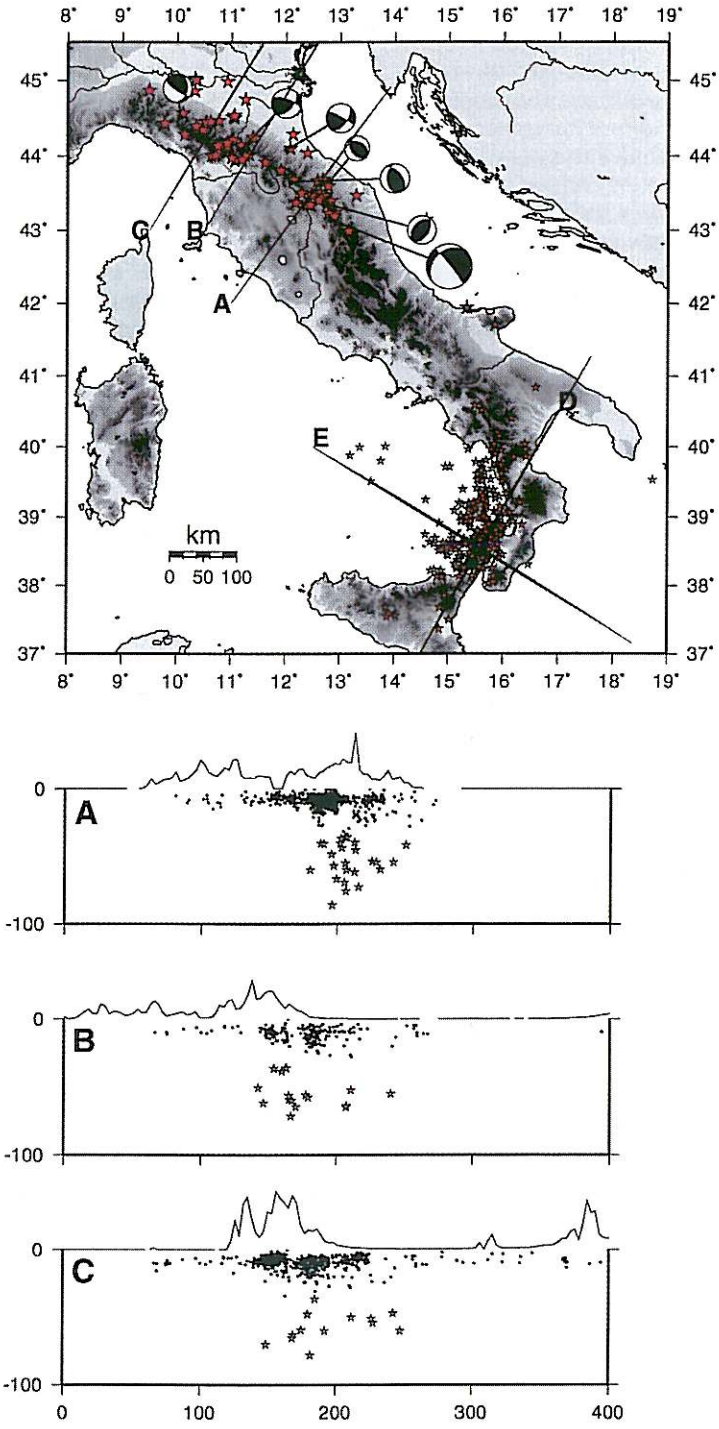
8° 9° 10° 11° 12° 13° 14° 15° 16° 17° 18° 19°
45° 44° 43° 42° 41° 40° 39° 38° 37°
A
B
C
D
E
km
0 50 100
0
-100
0
100
200
300
400

Fig. 1.

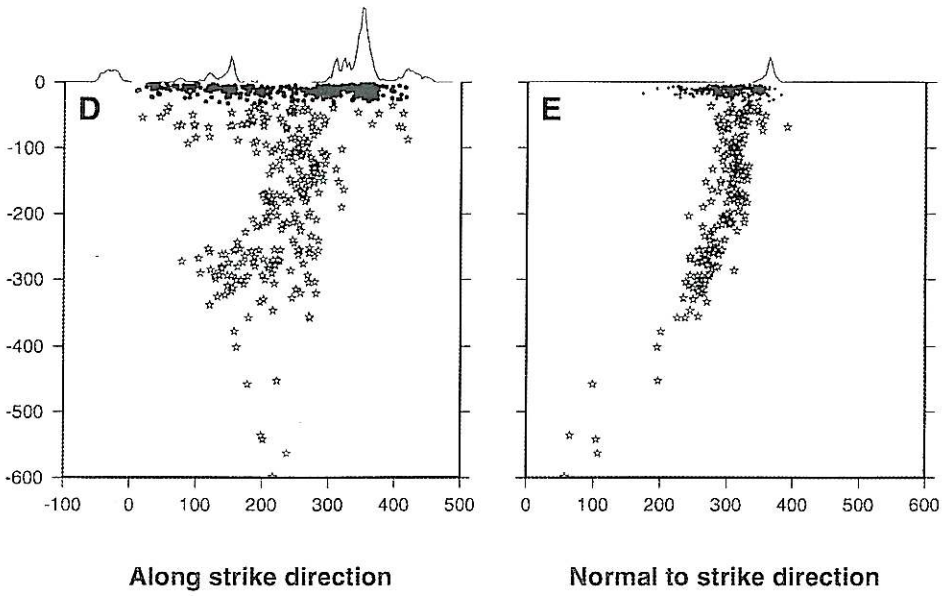

Fig. 1. Map showing the location of intermediate and deep earthquakes which have occurred in Italy from 1985 to the present. A, B and C are the traces of the southern, central and northernmost sections of the Northern Apennines subcrustal seismicity. The zones of projection do not overlap. D and E are along strike and perpendicular sections of the Tyrrhenian subduction zone. Topography is shown in all sections.

not been re-analysed but only critically evaluated. The larger magnitude fault plane solutions after 1977 come mostly from the Harvard CMT catalogue. The new solutions computed in this study, covering the time interval from 1995 to 1998, are constrained by the distribution of polarities, and for these magnitude the focal sphere is well covered by stations (fig. 2). In particular, the deep earthquakes are recorded by all the stations of the RSNC as can be seen from fig. 2 where, for a 4.0 magnitude event, the distribution of polarities portrays the upside-down familiar boot shape of the Italian territory fairly well. Table I reports the numerical features of the new fault plane solutions. The uncertainties in strike, dip, and rake of the fault plane solutions is within a few degrees. This is important because the uncertainties in the focal parameters, as well as in the scalar seismic moment, map directly in uncertainties in the strain tensor. Figure 3a shows the 57 fault plane solutions used in this study. Most of the solutions indicate

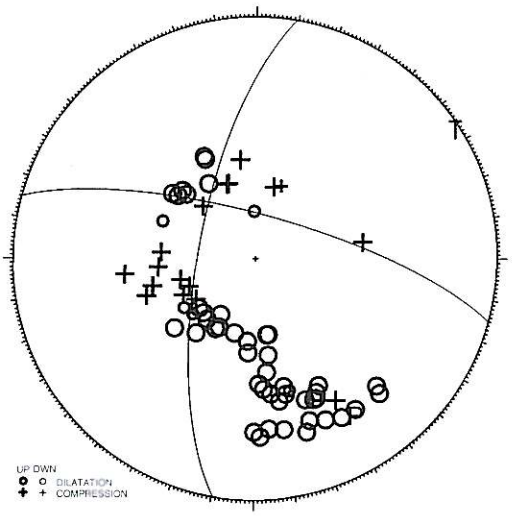

Fig. 2. Example of polarity distribution on a lower hemisphere projection for a small magnitude deep event of the Tyrrhenian zone.

Table I. Location and focal parameters of deep events of the Tyrrhenian subduction zone in 1996-1998 with M_b larger than 4.5. The M_b = 4.0 event has not been used in this paper.

Date	Latitude	Longitude	Depth	M_b	Strike	Dip	Rake
960121 12:17	39 58:98	13 16.88	539	4.7	300	85	180
960225 01:20	38 44.62	15 44.45	199	4.8	110	50	−150
960719 10:28	38 33.45	14 53.23	257	4.0	60	60	−90
961221 08:45	39 51.99	13 09.06	496	4.9	285	75	−160
980518 17:18	39 06.90	15 25.91	347	5.6	180	10	−140

normal faulting (fig. 3a) with planes trending generally towards the along strike direction of the slab. A few smaller magnitude solutions indicate strike slip and reverse mechanisms and they are located mainly above 150 km depth. The down-dip shortening is clearly visible in fig. 3b, revealed by the predominance of almost pure reverse solutions. Also the strike slip solutions have the *P* axes aligned with the down-dip direction. The trace of section in fig. 3b is the same as in fig. 1D and the focal mechanisms are here represented along the subduction plane (dipping towards NW at 70° from the horizontal). In the section perpendicular to the slab face (fig. 3c) the focal mechanisms appear as almost pure strike slip solutions, with the extensional *T* axis normal to the strike direction. As a first conclusion on the state of strain from fault plane solutions, one can point out that the shortening is confined in the down-dip direction while the lengthening is perpendicular to it. The inplane lengthening is very limited. In the 100-150 depth range, it is not clear if down-dip lengthening is predominant.

In order to calculate strain, the scalar seismic moment of the deep earthquakes must be evaluated. When not available from the standard CMT solutions (Dziewonski *et al.*, 1983), they have been obtained from magnitude by using the regression provided by Giardini (1988) for deep earthquakes. The total moment released by the deep earthquakes analysed in this study is equal to $5 \cdot 10^{26}$ dyne·cm, more than 90% of which is released in the 200-400 depth range, and mainly below 300 km depth (see also Frepoli *et al.*, 1996). The same feature is observed also without considering the largest 1938 event.

Fault plane solution and scalar seismic moment completely describe the moment tensor of an earthquake (Aki and Richards, 1980). A linear combination of seismic moment tensors provide an indication of average strain within a volume of interest (Kostrov, 1974). The analyses of the strain accommodated by earthquakes is restricted to a depth range between 100 km and 400 km, and to a time window of about 40 years, mainly for two reasons. The geometry of the slab from 100 down to 400 km can be approximated to a plane and the data set has been almost complete since the sixties. The depth range above 100 km depth has been excluded in this study because of the complex geometry, involving down-dip bending from subhorizontal to almost vertical beneath the Calabrian arc. Here, the observed strain is more likely related to the complex geometry rather then reflecting the interaction between the upper mantle and the slab itself (Nothard *et al.*, 1996). Similarly, below 400 km depth, recent tomographic images (Cimini, 1999) suggest a down-dip bending of the slab that could influence the strain pattern and for this reason it has been excluded. However, the strain in these depth ranges is substantially lower with respect to the 100-400 depth range and can be safely excluded from this analysis.

As a first step, the slab has been divided into cubic elements having sides of 50 km, the cumulative moment tensor has been computed for each element by taking into account the relevant earthquakes. Figure 4a shows the summed moment tensors in each cubic region.

When a fault plane solution is obtained from the summation of moment tensors, it may have

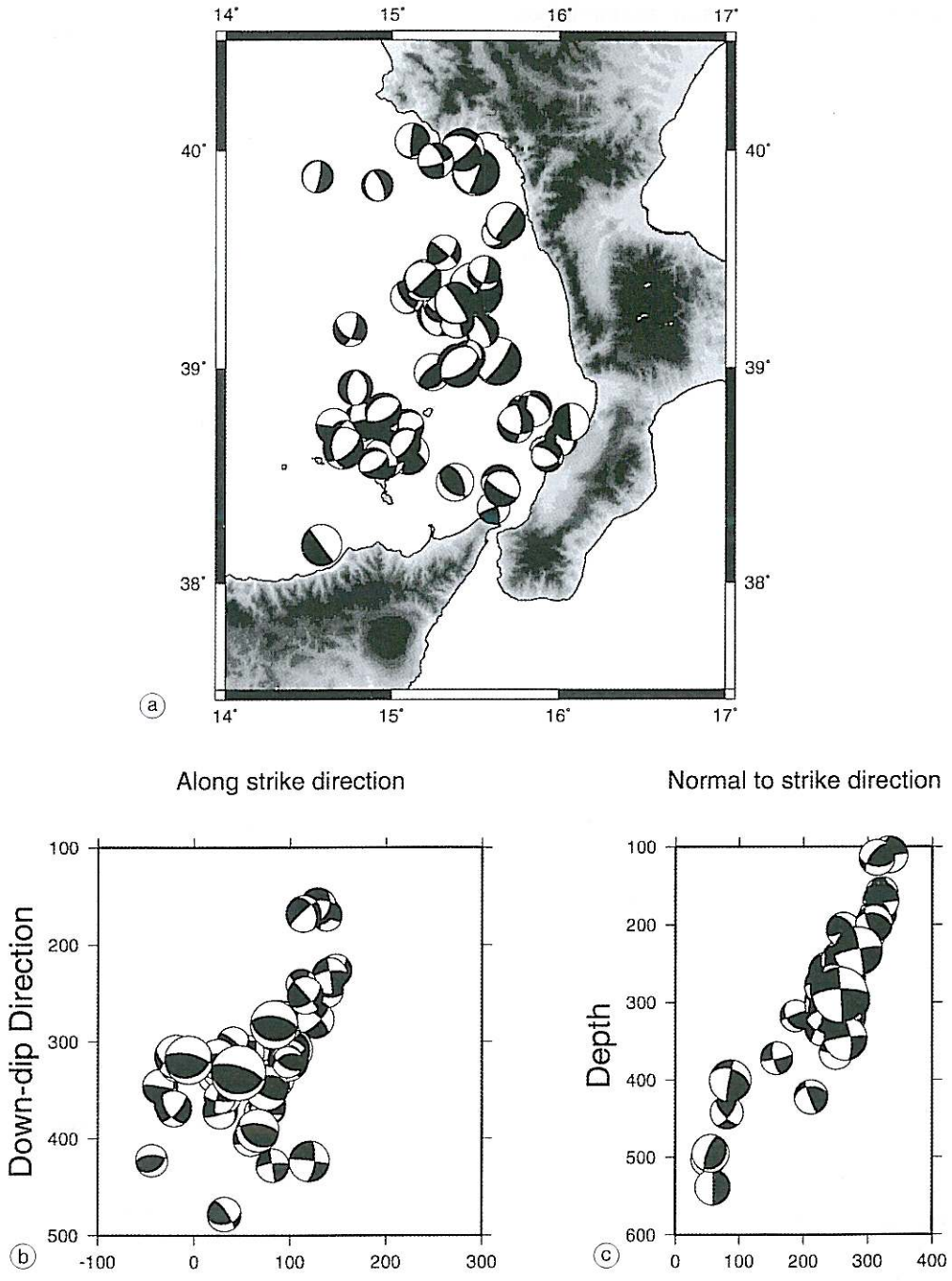

Fig. 3a-c. Available fault plane solutions for the Tyrrhenian deep earthquakes. a) Map view; b) projected on a 70° dipping plane in the along strike direction of the slab; c) perpendicular to the slab direction.

a large Compensated Linear Vector Dipole (CLVD) component. The CLVD component is the ratio between the intermediate and the largest eigenvalue of the moment tensor and ranges between 0, no CLVD component, and 0.5, pure CLVD mechanism (see Frohlich and Apperson, 1992 for an extensive review). Generally, first motion focal mechanisms are constrained to be double couple, however the CLVD component may rise from summation of double couple moment tensors depending on the magnitude difference of the each moment tensor and on their shape. This property of the moment tensors derive entirely from their geometric characteristics. The summation of moment tensors in each region of the Tyrrhenian subduction zone provides a limited CLVD component always below 0.1. Another property of summed moment tensors is that the sum of each scalar moment can be different from the scalar moment of the summed moment tensor (Frohlich and Apperson, 1992). The ratio between the two scalars is called *seismic consistency* (Cs), introduced by Frohlish and Apperson in 1992, and it is a measure of how different the individual moment tensors are. This ratio ranges between 0 and 1.0, perfectly consistent. Again, the seismic consistency is always near to 1 for the Southern Tyrrhenian earthquakes. Low values of CLVD component together with high values of seismic consistency observed in the summed moment tensors indicate that the strain is accommodated

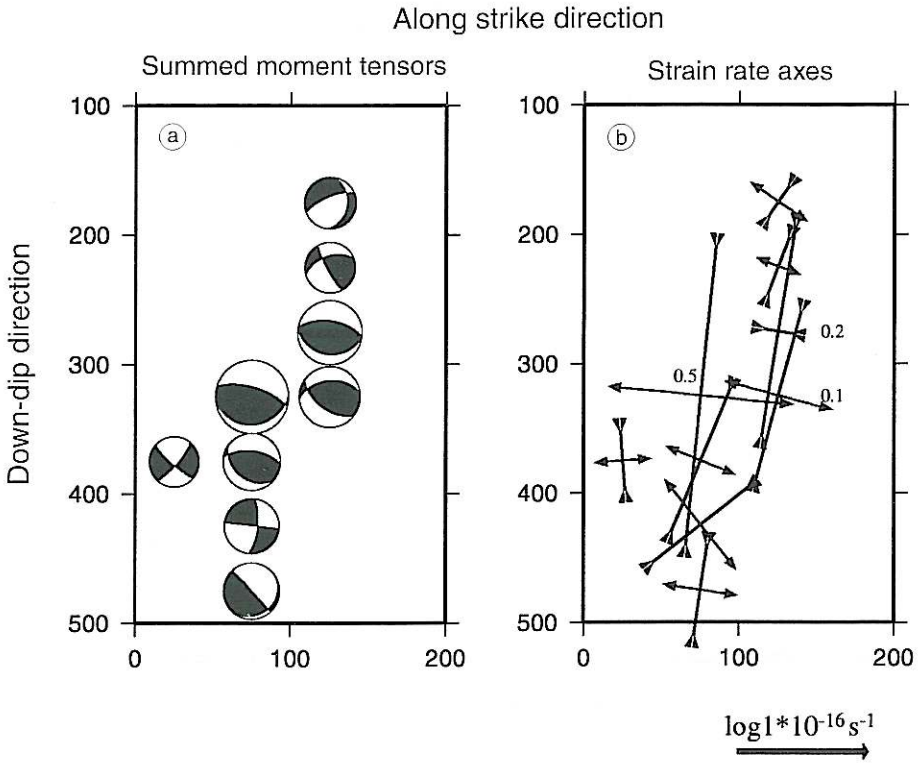

Fig. 4a,b. a) Summed moment tensor in each zone in which the slab has been divided. Fault plane solutions are scaled with magnitude; b) average seismic strain rate principal axes, inward arrows are compressional strain and outward arrows are extensional strain. Length is on log scale. Down-dip shortening (mm/yr) is shown in cubic regions when larger than 0.1 mm/yr.

by faults with almost the same orientation and sense of slip.

To calculate the average strain rate tensor, Kostrov' formula (1974) was used: an average seismogenic thickness of 50 km (derived from fig. 1E), a time interval of 40 years and a shear modulus of $8.5 \cdot 10^{11}$ dyne $\cdot$ cm^{-2} (Holt, 1995). Figure 4b show the principal strain rate axes along the slab face. As the magnitude of strain differs widely between volumes, a logarithmic scale is used to represent the principal axes. Black arrows are principal compressional strain rate axes while grey arrows are principal extensional strain rate axes. Two main features are evident in fig. 4b. The first is the increasing compressional strain rate from top to bottom of the slab, and the second is the small inplane extensional strain rate. The latter means that the extensional strain is confined in the direction perpendicular to the strike of the slab resulting in a thickening of the slab itself, that is what is generally observed in tomographic images. The first observation has a direct consequence on the average down-dip velocity.

5. Implications on the down-dip velocity

The basic drawback behind the possibility to infer velocity characteristics from strain rates is the assumption of constant ratio between the total energy release and that released by earthquakes (seismic efficiency) along the slab. Variation in the mechanical properties, thermobaric conditions, and phase transformations along the subducted slab clearly influence the depth distribution of earthquakes, depending on the age and vertical descent rate of the subducting slab (Kirby, 1995; Kirby *et al.*, 1996, Stein and Stein, 1996). These factors also influence the seismic efficiency but still in a poorly understood way. Nevertheless, in the papers of Holt (1995), and later in Nothard *et al.* (1996) it has been shown that the velocity field of the Tonga subduction zone, calculated from the strain pattern deduced from moment tensors of deep earthquakes in the planar portion of the Tonga slab, is consistent with the velocity of the Pacific plate with respect to Australia. Currently, this suggests that the variation in the mechanical properties and thermobaric conditions, and hence the assumption of constant seismic efficiency, could be of second order with respect to the strain raised by the interaction between the slab and the deep discontinuities.

The x coordinate axis was chosen so that the $\dot{\varepsilon}_{xx}$ component of the strain rate tensor is aligned with the down-dip direction of the slab. In this case, when averaged on the down-dip length of the grid used, the $\dot{\varepsilon}_{11}$ component is a measure of the average down-dip velocity gradient. Of course, the velocity we calculate is part of the total down-dip velocity of the descending slab, and in particular only that part related to the seismic deformation of the slab. Down-dip shortening implies that velocities decrease with depth and down-dip lengthening corresponds to an increase in velocity with depth. In the approach followed here, any indication on the lateral variation of the velocity with depth is missed, as the off-diagonal components of the strain rate tensor are not considered and the shortening rate in each cubic element from strain rate is calculated in the dip direction. Between 100 and 150 km depth the velocity slightly increases with depth, involving down-dip lengthening, but at greater depth it is always in down-dip shortening. In particular, the shortening rate is equal to ≈ 0.2 mm/yr between 250 and 300 km depth and equal to ≈ 0.5 mm/yr between 300 and 350 km of depth. This means that the velocity of the slab decreases towards the depth at least at those rates representing 10-15% of the total decreases of velocity used in geodynamic modelling (Giunchi *et al.*, 1996). The inclusion of the 1938 large event in the calculations does not increase these values to any great extent.

6. Discussion and conclusions

In this study we have calculated and here discuss strain pattern and the average down-dip velocity of the Southern Tyrrhenian subduction zone due to the occurrence of deep earthquakes. Although preliminary, in the sense that only one component of the velocity gradient tensor is determined, it is the first attempt to study the kinematics of the subducting Ionian lithosphere

in terms of velocity. The contribution from this study is primarily to corroborate what it can be inferred from tomographic images, that, in our view, are incomplete for assessing the kinematics of this region. Fault plane solutions have been widely used to study the kinematics of active regions because they are directly related to the strain accommodated by earthquakes.

The Southern Tyrrhenian subduction zone is in down-dip extension above 150 km depth and in down-dip shortening in the deepest part, increasing with depth. Here, the small inplane extensional strain rate implies a thickening of the slab between 300 and 400 km depth.

It is also enhanced that a large portion of the slab, between 100 and 250 km depth beneath the offshore of the Calabrian arc, is aseismic. This observation can be interpreted in at least two ways and both tomographic images and the description of the state of strain can help to better investigate this feature. The possible explanations refer to the evidence of an aseismic subduction or to a slab detached from its upper part. The most recent tomographic images are those reported in the paper by Cimini (1999), obtained using a non-linear inversion technique of direct and secondary teleseismic phases and a 3D minimum travel time ray tracing. Results show that the region where seismicity is absent is clearly characterised by strong positive velocity anomaly, indicating that the slab is still present at that depth range (Cimini, 1999). Moreover, it should be noted that in the seismic depth range between 100 and 250 km depth beneath Sicily (fig. 2d), there is a transition between down-dip extension and down-dip shortening and the strain rate is very low with respect to deeper regions. This depth range can be interpreted as a neutral down-dip stress zone, where the variation in the down-dip velocity is too low to permit large events to occur and those that may occur are too small and might be not recorded by the Italian national network. We conclude suggesting that the lack of seismicity can be referred to the evidence of an aseismic subduction.

Finally, the question is to understand why the slab decreases in velocity in the way it does and how we can explain the seismicity distribution with depth and its state of strain. Such features, both velocity, depth distribution of seismicity and down-dip compression everywhere below 200 km, suggest, agreeing with worldwide observations of slab behaviour (Vassiliu and Hager, 1988), the influence of the 670 km depth viscosity contrast in the difficult penetration of the slab in the deepest part of the upper mantle.

A simple model of sinking slab subject only to gravitational forces reaching the 670 discontinuity produces a pattern of strain field completely in agreement with our observations (Vassiliu and Hager, 1988). In particular, the strain field is in down-dip tension above 200 km depth, a neutral stress zone and a peak below 300 km depth in down-dip compression down to the 670 km discontinuity.

Acknowledgements

I wish to thank Antonio Piersanti for useful suggestions. I also thank Claudio Faccenna and an anonymous referee for their constructive review. This work has been partially founded by ASI-ARS contract 1999.

REFERENCES

AKI, K. and P. RICHARDS (1980): *Quantitative Seismology: Theory and Methods* (W.H. Freeman and Company, San Francisco), 2 vols.

AMATO, A., B. ALESSANDRINI, G.B. CIMINI, A. FREPOLI and G. SELVAGGI (1993): Active and remnant subducted slabs beneath Italy: evidence from seismic tomography and seismicity, *Ann. Geofis.*, **36** (2), 201-214.

ANDERSON, H. and J. JACKSON (1987): The deep seismicity of the Tyrrhenian Sea, *Geophys. J. R. Astron. Soc.*, **91**, 613-637.

CIMINI, G.B. (1999): P-wave deep velocity structure of the Southern Tyrrhenian subduction zone from non-linear teleseismic traveltime tomography, *Geophys. Res. Lett.*, **26** (24), 3709-3712.

DOGLIONI, C., E. GUEGUEN, F. SABAT and M. FERNANDEZ (1997): The Western Mediterranean extensional basins and the Alpine orogen, *Terra Nova*, **9** (3), 109-112.

DZIEWONSKI, A.M., A. FRIEDMAN, D. GIARDINI and J.H. WOODHOUSE (1983): Global seismicity of 1982: centroid moment tensor solutions for 308 earthquakes, *Phys. Earth Planet. Int.*, **53**, 17-45.

ENGLAND, P. and G. HOUSEMAN (1986): Finite strain calculations of continental deformation, 2, comparison with the India-Asia collision zone, *J. Geophys. Res.*, **91**, 3664-3676.

FREPOLI, A., G. SELVAGGI, C. CHIARABBA and A. AMATO (1996): State of stress in the Southern Tyrrhenian subduction zone from fault plane solutions, *Geophys. J. Int.*, **125**, 879-891.

FROHLICH, C. and K.D. APPERSON (1992): Earthquake focal mechanisms, moment tensors, and the consistency of seismic activity near plate boundaries, *Tectonics*, **11** (2), 279-296.

FUNG, Y.C. (1965): *Foundations of Solid Mechanics* (Prentice-Hall, Englewood Cliffs, N.J.), pp. 525.

GASPARINI, C., G. IANNACCONE, P. SCANDONE and R. SCARPA (1982): Seismotectonics of the Calabrian arc, *Tectonophysics*, **84**, 267-286.

GIARDINI, D. (1988): Frequency distribution and quantification of deep earthquakes, *J. Geophys. Res.*, **93**, 2095-2105.

GIARDINI, D. and M. VELONÀ (1990): The deep seismicity of the Tyrrhenian Sea, *Terra Nova*, **3**, 57-64.

GIUNCHI, C., R. SABADINI, E. BOSCHI and P. GASPERINI (1996): Dynamic models of subduction: geophysical and geological evidence in the Tyrrhenian Sea, *Geophys. J. Int.*, **126**, 555-578.

HAINES, A.J. (1982): Calculating velocity fields across plate boundaries from observed shear rates, *Geophys. J. R. Astron. Soc.*, **68**, 203-209.

HOLT, W.E. (1995): Flow fields within the Tonga slab determined from the moment tensors of deep earthquakes, *Geophys. Res. Lett.*, **22** (8), 989-992.

KIRBY, S.H. (1995): Interslab earthquakes and phase changes in subducting lithosphere, *Suppl. Rev. Geophys.*, 287-297.

KIRBY, S.H., S. STEIN, E.A. OKAL and D.C. RUBIE (1996): Metastable phase transformation and deep earthquakes in subducting oceanic lithosphere, *Rev. Geophys.*, **34**, 261-306.

KLEIN, F.W. (1989): Hypoinverse, a program for Vax computers to solve for earthquake location and magnitude, *U.S. Geol. Surv. Open File Rep.*, 89-314, 6/89 version.

KOSTROV, V.V. (1974): Seismic moment and energy of earthquakes, and seismic flow of rock, *Izv. Acad. Sci. USSR Phys. Solid Earth*, **1**, 23-44.

IANNACCONE, G., G. SCARCELLA and R. SCARPA (1985): Subduction zone geometry and stress patterns in the Tyrrhenian Sea, *Pageoph*, **123**, 819-836.

JACKSON, J. and D. MCKENZIE (1988): The relationship between plate motion and seismic moment tensor, and the rates of active deformation in the Mediterranean and Middle East, *Geophys. J.*, **93**, 45-73.

LUCENTE, F.P., C. CHIARABBA, G.B. CIMINI and D. GIARDINI (1999): Tomographic constraints on the geodynamic evolution of the Italian region, *J. Geophys., Res.*, **104** (B9), 20307-20327.

MCKENZIE, D. and J. JACKSON (1983): The relation between strain rates, crustal thickening, paleomagnetism, finite strain and fault movements within a deforming zone, *Earth Planet. Sci. Lett.*, **65**, 182-202

NOTHARD, S., J. HAINES, J. JACKSON and B. HOLT (1996): Distributed deformation in the subduction lithosphere at Tonga, *Geophys. J. Int.*, **127**, 328-338.

SELVAGGI, G. and A. AMATO (1992): Subcrustal earthquakes in the Northern Apennines (Italy): evidence for a still active subduction?, *Geophys. Res. Lett.*, **19** (21), 2127-2130.

SELVAGGI, G. and C. CHIARABBA (1995): Seismicity and *P*-wave velocity image of the Southern Tyrrhenian subduction zone, *Geophys. J. Int.*, **121**, 818-826.

SPAKMAN, W., S. VAN DER LEE and R. VAN DER HILST (1993): Travel-time tomography of the European-Mediterranean mantle down to 1400 km, *Phys. Earth Planet. Inter.*, **79**, 3-74.

STEIN, S. and C.A. STEIN (1996): Thermo-mechanical evolution of oceanic lithosphere: implications for the subduction process and deep earthquakes, in *Subduc-tion Top to Bottom*, edited by G. BEBOUT, D.W. SCHOLL, S.H. KIRBY and J.P. PLATT, *Am. Geophys. Un.*, 1-17

VASSILIOU, M.S. and B.H. HAGER (1988): Subduction zone earthquakes and stress in slabs, *Pageoph*, **128** (3/4), 547-605.

(received November 29, 2000;
accepted February 7, 2001)